NMRlipids IV: Headgroup & glycerol backbone structures, and cation binding in bilayers with PS lipids

O. H. Samuli Ollila[1, 2, *]

[1]*Institute of Organic Chemistry and Biochemistry, Academy of Sciences of the Czech Republic, Prague 6, Czech Republic*
[2]*Institute of Biotechnology, University of Helsinki*
(Dated: March 8, 2018)

Primarily measured but also simulated NMR order parameters will be collected also for other than phophatidylcholine (these are discussed in NMRlipids I) headgroup. The information will be used to understand structural differences between different lipid molecules in bilayers.

INTRODUCTION

Phosphatidylserine (PS) is the most common negatively charged lipid in eykaryotic membranes. PS lipids compose 8.5% of total lipid weight of erythrocytes, but the abundance varies between different organelles up to 25-35% in plasma membrane [1–3]. Despite of the relatively low abundance, PS lipids are important signaling molecules. They interact with signaling proteins [2], regulate surface charge and protein localization [4], and induce protein aggregation [5, 6]. Some domains spesifically interact PS lipids, while others are attracted by general electrostatics and the binding can be regulated by calcium [2]. Therefore, the structural details of lipid headgroups and the details of calcium binding are crucial for the PS mediated signaling processes.

The structure of PS lipid headgroups and their interactions with ions have been studied with various experimental methods and theoretical techniques [7?, 8]. However, the consesus has not been reached due to the difficulties to interpret the experimental data [?] and the inaccuracies in simulation models at the headgroup region [9–11]. Some studies propose that the negatively charged lipids attract cations only due to the increase of local concentration in the vicinity of membranes and that the binding constant of cations is similar to zwitterionic and negatively charged lipids [12?, 13]. On the other hand, some studies propose specific binding of calcium directly to PS lipid headgroups [14?, 15], The NMR data proposes that the PS headgroup is more rigid than PC,PE or PG headgroups, but more detailed interperetation has not been done.

Headgroup and glycerol backbone C-H bond order parameters calculated from MD simulations have been recently used to interpret the lipid structures in NMR experiments and to validate lipid structure and ion binding in simulations of PC lipid bilayers [9–11, 16]. In this work we apply this approach to PS lipid headgroup in order to elucidate the structural details and ion binding to negatively charged lipids. The results are expected to elucidate also PS mediated signalling events because glycerol backbone and headgroup structure and behaviour are similar in model membranes and in bacteria [12, 17, 18].
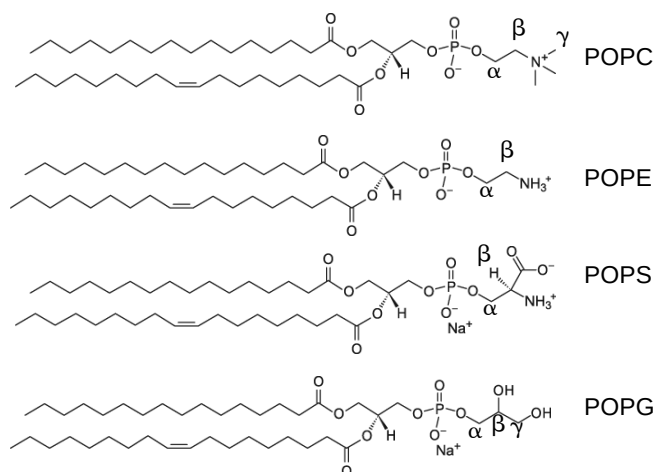

FIG. 1: Chemical structures and labels for the headgroup carbons.

METHODS

Solid state NMR experiments

The experimental protocol is the same used in Ref. 16. **1.Some basic details should be given.**

Molecular dynamics simulations

Molecular dynamics simulation data was collected with Open Collaboration method. The simulated systems are listed in Table I. The simulation details are in SI or in references in the table.

RESULTS AND DISCUSSION

Headgroup and glycerol backbone order parameters measured from POPS lipid bilayer

Figs. 2 and 3 summarize the experimental NMR results for POPS bilayer sample. **13.New figure, probably combining Figs. 2 and 3, should be done. This discussion to be finished after this.**

TABLE I: List of MD simulations. The salt concentrations calculated as [salt]=$N_c \times$[water]$/N_w$, where [water]$= 55.5$ M. CKP1 referes to the version with Berger/chiu NH3 charges compatible with Berger and CKP2 to the version with more Gromos compatible version.

lipid/counter-ions	force field for lipids / ions	NaCl (mM)	CaCl$_2$ (mM)	^{a}N$_l$	^{b}N$_w$	^{c}N$_c$	^{d}T (K)	^{e}t$_{sim}$(ns)	^{f}t$_{anal}$ (ns)	^{g}files
DOPS/Na$^+$	CHARMM36 [?] 2.	0	0	128	4480	0	303	500	100	[19]
DOPS/Na$^+$	CHARMM36ua [?] 3.	0	0	128	4480	0	303	500	100	[20]
DOPS/Na$^+$	Slipids [21]	0	0	128	4480	0	303	500	100	[22]
DOPS/Na$^+$	Slipids [21]	0	0	288	11232	0	303	200	100	[23]
DOPS/Na$^+$	Berger [24]	0	0	128	4480	0	303	500	100	[25]
DOPS/Na$^+$	GROMOS-CKP1 [?] 4.	0	0	128	4480	0	303	500	100	[26]
DOPS/Na$^+$	GROMOS-CKP2 [?] 5.	0	0	128	4480	0	303	500	100	[27]
DOPS/Na$^+$	lipid17 [?]	0	0	?	?	?	?	?	?	[?]
POPS/Na$^+$	CHARMM36 [?] 6.	0	0	128	4480	0	298	500	100	[28]
POPS/K$^+$	CHARMM36 [?] 7.	0	0	128	4480	0	298	500	100	[29]
POPS/Na$^+$	CHARMM36ua [?] 8.	0	0	128	4480	0	298	500	100	[30]
POPS/Na$^+$	Slipids [21]	0	0	128	4480	0	298	500	100	[31]
POPS/Na$^+$	Berger [?]	0	0	128	4480	0	298	500	100	[32]
POPS/Na$^+$	MacRog [33]	0	0	128	5120	0	298	200	100	[34]
POPS/Na$^+$	GROMOS-CKP1 [?] 9.	0	0	128	4480	0	298	500	100	[35]
POPS/Na$^+$	GROMOS-CKP2 [?] 10.	0	0	128	4480	0	298	500	100	[36]
POPS/Na$^+$	lipid17 [?]	0	0	?	?	?	?	?	?	?
POPC:POPS (5:1)/K$^+$	CHARMM36 [37?] 11.	0	0	110:22	4935	0	298	100	100 12.	[38]

^{a}Number of lipid molecules with largest mole fraction
^{b}Number of water molecules
^{c}Number of additional cations
^{d}Simulation temperature
^{e}Total simulation time
^{f}Time used for analysis
^{g}Reference for simulation files

The headgroup and glycerol backbone order parameters of POPS measured in this work are compared to the literature values of DOPS [40] and POPC [41] in Fig. 4. Our results for POPS are in good agreement with the previously reported values for DOPS measured with ^{2}H NMR. Significant differences are observed between PC and PS lipids, especially at the headgroup region. Previous discussions in the literature have concluded that glycerol backbone structure is largely similar in PC, PE, PG and PS lipids [17]. The headgroup region was found to be similar in PC, PE and PG lipid (assuming that the signs of PE and PG order parameters are the same as in PC), while the PS headgroup was suggested to be more rigid [42, 43]. The detailed structural differences between the headgroups is, however, not known.

Headgroup and glycerol backbone in simulations of PS lipid bilayers without additional ions

The headgroup order parameters of DOPS and POPS bilayers from different simulation models are compared with the experimental data in Fig. 5. In line with the previous study for PC lipids [9], the glycerol backbone order parameters in CHARMM36 roughly agree with the experimental data, while

significant discrepancies for glycerol backbone carbons are observed in other models. 21.Discussion to be finished once all the results are in the plot.

Based on the subjective ranking shown in Fig. 6, the CHARMM36 is the best performing model for both lipids. However, none of the tested models give a satisfactory agreement with experiments for the headgroup order paramaters of PS lipids. The total deviation from the experiments (Σ in Fig. 6) for the best performing CHARMM36 model is larger for PS lipids (8) than for PC (3) [9]. Therefore the interpretation of structural details of PS headgroup or differences between PC and PS lipids is very challenging from the current MD simulation models. Figures 16 and 17 show dihedral angle distributions calculated from different models. The glycerol backbone structures from CHARMM36 and Slipids simulations visualized in Fig. 7 reveal the missing structures in Slipids model, which probably lead to the incorrect order parameters. For the headgroup α and β carbon order parameters of PS lipids, the tested models perform less well than for PC headgroup in previous study [9]. 22.Discussion will be finished when we have all the data in Figs. 5, 16 and 17. One possible conclusion could be the following: The main differences between the models in the headgroup region are observed for dihedrals C12-C11-O12-P and C11-C12-C13-O1A. CHARMM36, CHARMM36UA and Slipids give very similar results to the dihedral C11-C12-C13-O1A, which is

FIG. 2: (a) The headgroup region of the INEPT spectrum where alpha and beta are identified. (b) The R-PDLF slices for alpha and beta showing one single splitting for beta (which gives an order parameter equal to 0.12), and for alpha a superposition of a large splitting (order parameter equal to 0.09) and a very small splitting which cannot resolved with the available resolution. (c) Points with error bars are the experimental SDROSS data. The thick lines are SIMPSON simulations. The S-DROSS slice for beta clearly shows that the order parameter is negative, which is confirmed by SIMPSON simulations using the order parameter value of -0.12. The S-DROSS slice for alpha suggests that the higher order parameter is positive and the deviation towards negative values in the longer t1 times suggests that the smaller order parameter is negative. This is confirmed by SIMPSON simulation using value of 0.09 for the larger alpha order parameter and the value of -0.02 for smaller (black curve). The value for the smaller alpha order parameter for SIMPSON calculation was taken from Fig 3 in Ref. 39, because resolution in 13C NMR experiments was nor high enough to determine numerical value for this. The S-DROSS curve from SIMPSON simulation with positive value for the smaller order parameter gave did not agree with experiments (dashed grey), confirming the interpretation that the smaller order parameter is negative.

14.Maybe we should combine this with 3

close to the β-carbon. The order parameters of β-carbons for these three models
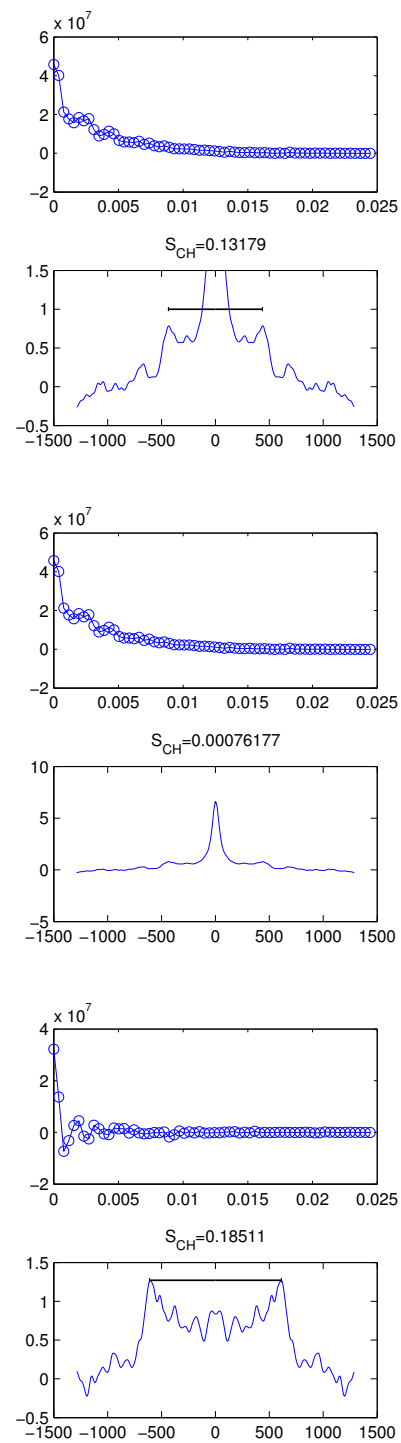
FIG. 3: R-PDFL slices for gycerol backbone carbons.

15.We need nicer figure for this data. Maybe combine with 2

16.What are the top figures actually?

are in best argeement with the experiments in figure 5. On the other hand, Gromos-CKP models give better order parameters for α-carbon than Slipids, CHARMM36 or CHARMM36UA. In conclusion, the suggestion would be that the single peak

FIG. 4: Headgroup and glycerol backbone order parameters of POPS measured in this work compared with values for DOPS (^{2}H NMR, 0.1M of NaCl) [40] and POPC (^{13}C NMR) [41] from literature. Signs for PS order parameters as measured in this work and signs for PC as measured in Refs [16 ?].

for observed at 120 degrees in CHARMMs and Slipids would be more realistic for C11-C12-C13-O1A dihedral, while the single peak at 180 degrees observed in CKP models and in Berger would be most realistic for C12-C11-O12-P dihedral.

Since systems with negatively charged PS lipids always contain counterions and the ion binding presumably affects the PS headgroup order parameters, the discussion of ion binding affinity and headgroup structure cannot be separated as done previously for PC lipids [9, 10]. The density profiles of counterions along membrane normal from different simulations are shown in Fig. 8. Significant differences are observed in counterion densities between different simulation models. **23.We should try to figure out which one of these are more realistic. One option could be to use PS headgroup order parameter data measured as a function of NaCl [44]. Another approach could be to use the area per molecule, which is suggested to depend on the binding affinity of counterions [24, 45, 46]. The experimental value for area per molecule is available at [47].**

Headgroup structure in PS and PC mixtures

Cellular membranes often compose of mixtures of zwitterionic and negatively charged lipids. The response of PC headgroup to mixtures of differently charged lipids are collected from different experiments in Fig. 13. As expected from the electrometer concept [48], the headgroup order parameters increase with the addition of negatively charged PS and PG lipids, decrease when mixed with positively charged surfactants and are less affected by the addition of zwitterionic PE lipids or cholesterol. In addition to the results summarized in Fig. 13, also mixtures of PC with negatively charged PI, CL, PA, and zwitterionic SM follow the eletrometer concept [18].
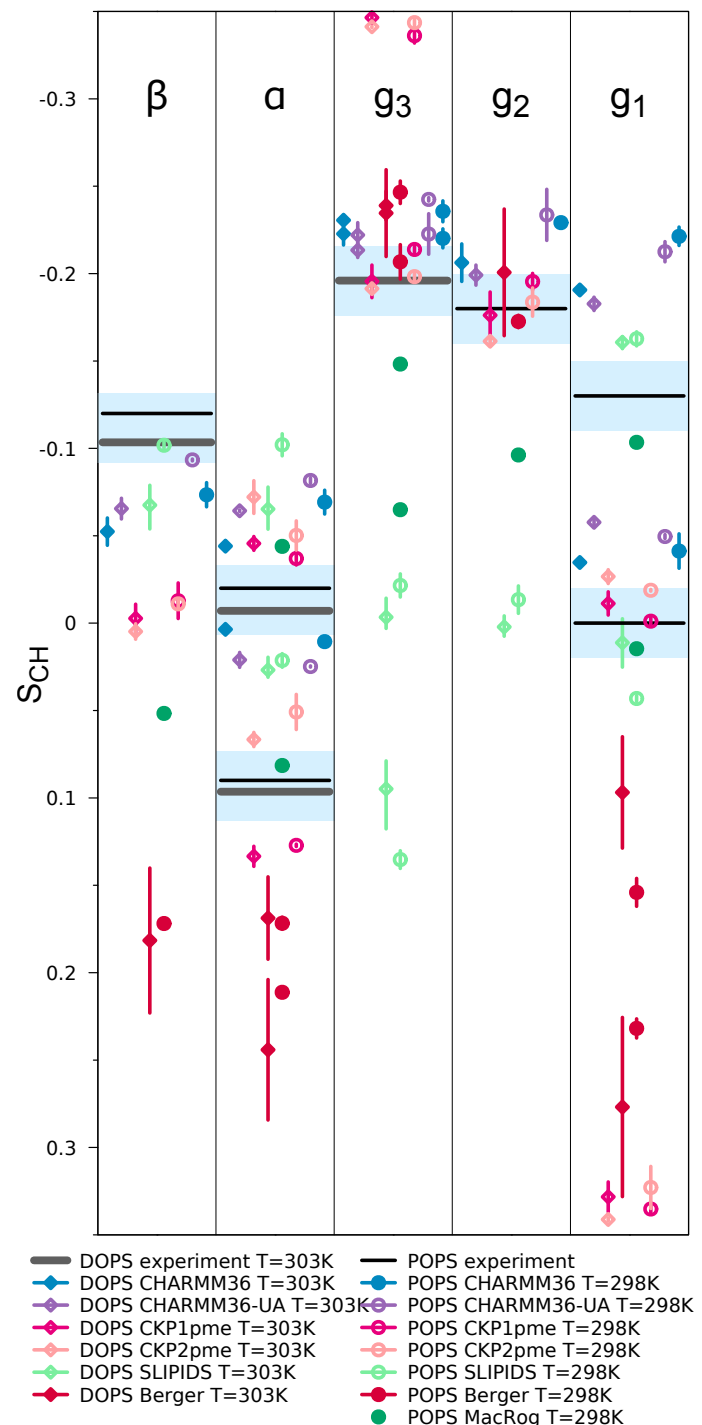
Fig. 9 shows the PC and PS headgroup order parameters

FIG. 5: Order parameters for PS headgroup and glycerol backbone from simulations with different models and experiments without CaCl$_2$ Experimental data from [40] contains 0.1M of NaCl. Signs are taken from experiments for POPS described in Supplementary Information. The vertical bars shown for most computational values are not error bars, but demonstrate that for these systems we had at least two data sets; the ends of the bars mark the extreme values from the sets, and the dot marks their measurement-time-weighted average.

17.In table I: "CKP1 referes to the version with Berger/chiu NH3 charges compatible with Berger and CKP2 to the version with more Gromos compatible version." Is this correct also in this figure?

18.Lipid17 results should be added.

19.We should also add CHARMM36 POPS ran with K counterions: https://github.com/NMRLipids/NMRlipidsIVotherHGs/issues/1#issuecomment-308570874

	β	α	g₃	g₂	g₁	Σ
CHARMM 36	M	M F	M	M	M F	8
CHARMM 36-UA	M	M	M	M	M F	8
GROMOS-CKP1	**M**	M F	**M F**		**M F**	14
GROMOS-CKP2	**M**	M F	**M F**		**M F**	14
Slipid	M	**M**	**M F**	**M**	M F	14
Berger	**M**	**M F**	M F	M	**M F**	15

FIG. 6: Rough subjective ranking of force fields based on Figure 5. Here M indicates a magnitude problem, F a forking problem; letter size increases with problem severity. Color scheme: within experimental error (dark green), almost within experimental error (light green), clear deviation from experiments (light red), and major deviation from experiments (dark red). The Σ-column shows the total deviation of the force field, when individual carbons are given weights of 0 (matches experiment), 1, 2, and 4 (major deviation). For full details of the assessment, see Supplementary Information.
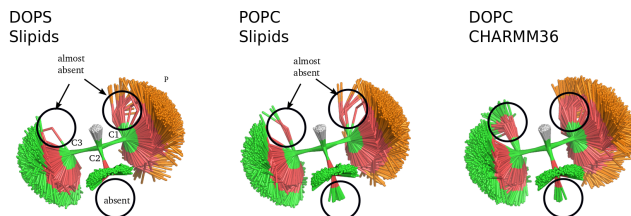
FIG. 7: Snapshots overlayed from different simulations for glycerol backbone region by Pavel Buslaev.

from POPC:POPS mixtures with various mole fractions from simulations and experiments [7, 18]. The experimentally observed increase of PC headgroup order parameters with the increasing amount of negatively charged PS lipid is reproduced in MacRog simulations with potassium counterions, but not in CHARMM36 simulations with potassium or sodium conterions. The results can be understood from the counterion density distributions shown in Fig. 10. Both counterions are more strongly bound to bilayers in CHARMM36 simulations than potassium in MacRog simulation. The cation binding probably neutralizes the effect of negatively charged lipids in CHARMM36 simulations, while the weaker binding of potassium in MacRog simulations enables the increase of order pa-
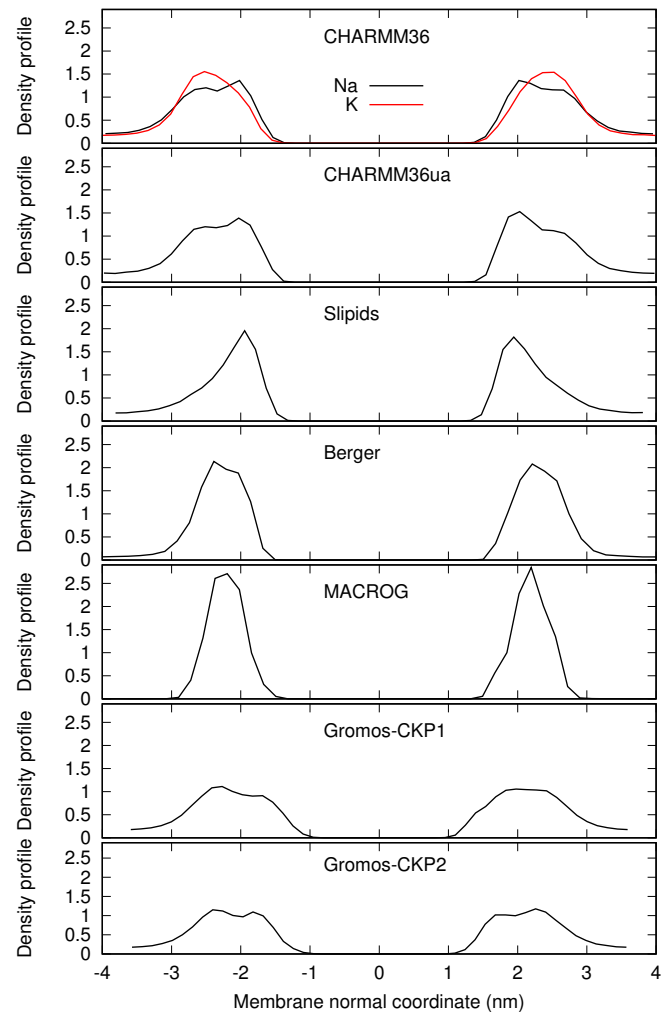
FIG. 8: Counterion densities of POPS lipid bilayer along the membrane normal from simulations with different force fields.

rameters with the added amount of PS.

Also the headgroup order parameters of POPS mixed with varying amounts of POPC from simulations and experiments [7, 49] are shown in Fig. 9. The β-carbon order parameter of POPS slightly decreases and positive order parameter of α-carbon slightly increases with increasing amount of PS lipids. This may indicate increasing order of the headgroup. It should be, however, noted that the experimental data for pure POPS and POPC/POPS mixture come from different experimental sets, 13C NMR in this work and 2H NMR from Ref. 7, respectively. Therefore the accuracy of the order parameter change is not as high as typically in the measurements of order parameter changes, see discussion about qualitative and quantitative accuracy in Ref. 11. The changes of PS headgroup order parameters are not reproduced by the tested simulation models. The β-carbon order parameter increase with increasing amount of PS in CHARMM36 and MacRog simulations in contrast to the experimental data. The smaller
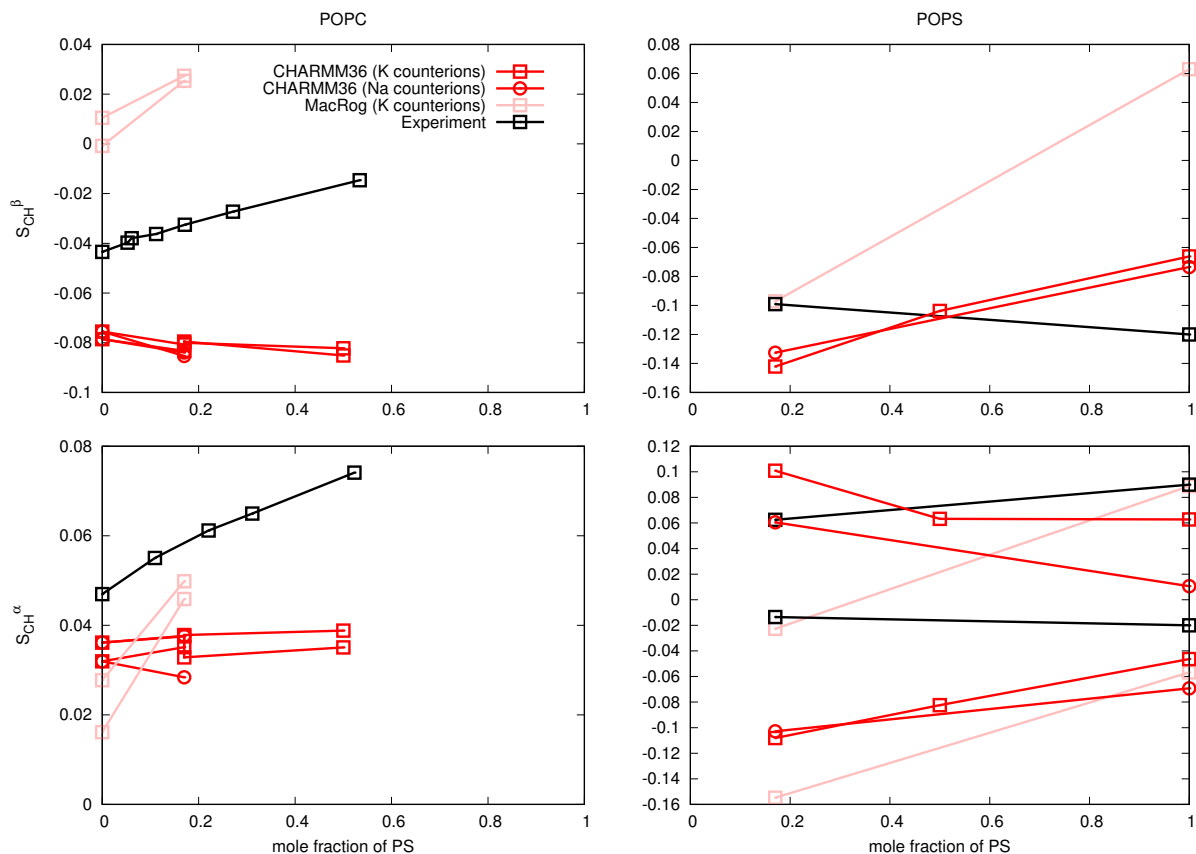
FIG. 9: Headgroup order parameters from PC:PS mixtures from different simulation models and experiments. Left panel shows the PC headgroup order parameters (experimental results from Ref. 18, signs are determined as discussed in [9, 11]). Rigth panel shows PS headgroup order parameters (experimental result for pure POPS measured in this work at 298K, experimental result for mixture from Ref. 7 at 298K). Counterions in expriments are sodium, while potassium is used in simulations. Using sodium in simulations do not have a significant effect.

24.Simulation of CHARMM36 at 298K should be maybe rerun with Gromacs 5.

25.We need results also from other than CHARMM36 force field.

α-carbon order parameter increase in both simulation models with increasing amount of PS, while it is almost unchanged in experiments. The larger α-carbon order parameter increase in MacRog and decrease in CHARMM36 with increasing amount of PS, both model exhibiting a poor agreement with experiments. Signifincant improvement in the MD simulation models are needed to interpret the PS headgroup structures and mutual interactions with PC lipids.

Ca^{2+} binding affinity in bilayers with negatively charged PS lipids

The headgroup order parameters of PC lipids decrease proportionally to the bound positive charge in to a bilayer [10, 48] and can be therefore used to measure the ion binding affinity. This molecular electrometer concept can be also applied to lipid bilayers with mixtures of PC and negatively charged lipids [7, 49, 50] (see Fig. 14).

The headgroup order parameter changes of POPC and POPS from POPC:POPS (5:1) bilayers as a function of

Ca2+ concentration from different simulations and experiments [7] are shown in Fig. 11. The results suggest that Ca2+ ions clearly overbind in simulations with MacRog model, as expected from previous results for PC lipid bilayers [10]. It should be noted, however, that the lowest concentration (100mM) gives a good agreemet with experiments **26.Should be analyze/discuss this further?**. Surprisingly, the calcium binding seems to be too weak CHARMM36 simulations **27.This is most likely due to the new interactions added to CHARMM-GUI: http://nmrlipids.blogspot.com/2017/12/nmrlipids-iv-current-status-and.html?showComment=1519913688317#c5312059274016196300** . The density profiles of Ca2+ from the simulations are shown in Fig. 12. **28.More simulation data for systems with PS lipids and CaCl$_2$ would be probably useful**

Also the order parameters of PS headgroup as a function of CaCl$_2$ concentration are shown in Fig. 11. The order parameters exhibit a strong dependence small CaCl$_2$ concentrations with a rapid saturation. The changes of PS headgroup order parameters with added CaCl$_2$ are overestimated in both simulation models. The response of β-carbon order param-
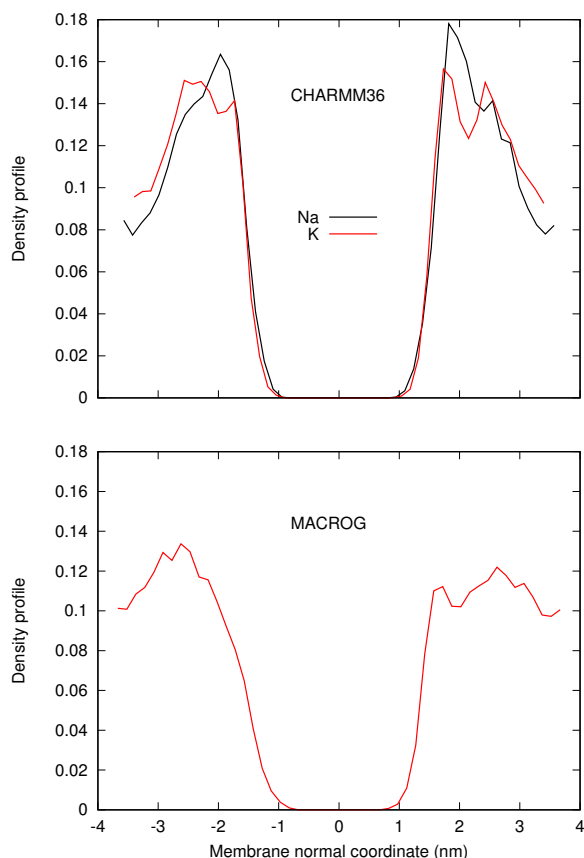
FIG. 10: Counterion density distributions from PC:PS mixtures.

Simulated systems

PC lipid headgroup response to different mixtures in experiments

As shown in Fig. 13, order parameters of PC headgroup behave in various lipid mixtures as expected from the electrometer concept [18, 48], i.e., order parameters increase when anionic lipids are mixed with PC and decrease with cationic surfactants. The changes with the addition of neutral lipids is significantly smaller.

Cation binding affinity to lipid bilayers with different amount of charge

Before using the headgroup order parameters to compare ion binding affinity between simulations and experiments, it is important to quantify the response of the order parameters to the bound charge in simulations. The response of headgroup order parameters to the fixed amount of cationic surfactants in POPC bilayer is compared between simulations and experiments [51] In Fig. 15. The figure shows that the order parameters are too sensitive to bound charge in Lipid14 model, while CHARMM36 is in better agreement with experiments. This has to be taken into account when analysin the binding affinities.

eter could be interpreted qualitatively correct in simulations, but the general agreement with experiments is not sufficient to use simulations to interpret the response of PS headgroup to the added CaCl$_2$.

Dihedrals

CONCLUSIONS

Dihedrals
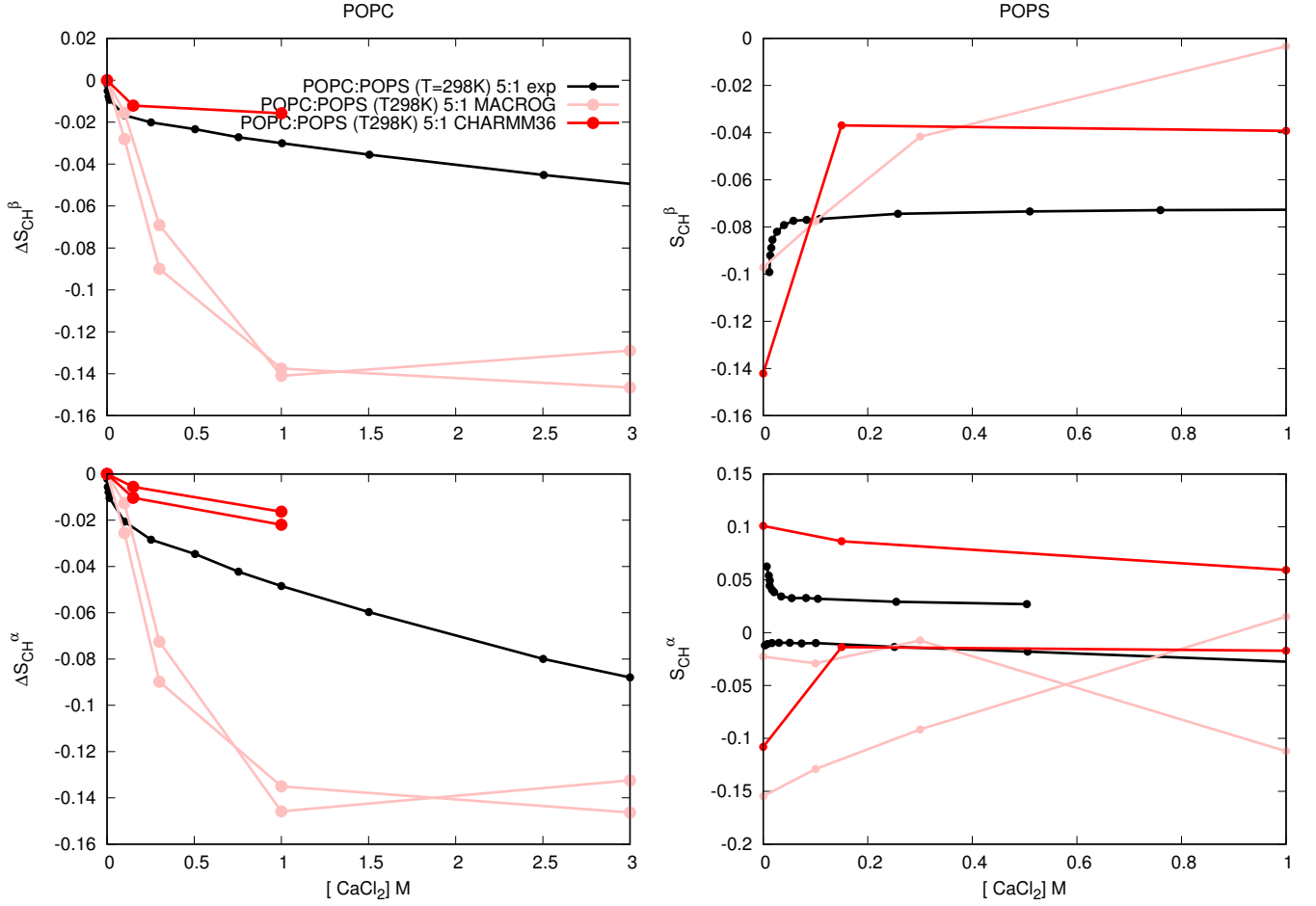
FIG. 11: POPC (left) and POPS (right) headgroup order parameters in lipid bilayer with POPC:POPS (5:1) mixture as a function CaCl$_2$ concentration from experiments [7] and different simulations.

Details of the rough subjective force field ranking (Fig. 6)

The assessment was based fully on the Fig. 5. First, for each carbon (the columns in Fig. 5) in each force field (the rows), we looked separately at deviations in magnitude and forking.

Magnitude deviations, i.e., how close to the experimentally obtained C–H order parameters (OPs) the force-field-produced OPs were. For each carbon, the following 5-step scale was used:

>   **0 ( ):** More than half of all the calculated OPs (that is, of all different hydrogens in all different lipids) were within the *subjective sweet spots* (SSP, blue-shaded areas in Fig. 5).
>
>   **1 (M):** All the calculated OPs were < 0.03 units away from the SSP.
>
>   **2 (M):** All the calculated OPs were < 0.05 units away from the SSP.
>
>   **3 (M):** All the calculated OPs were < 0.10 units away from the SSP.

4 (M): Some of the calculated OPs were > 0.10 units away from the SSP.

Forking deviations, i.e., how well the difference in order parameters of two hydrogens attached to a given carbon matched that obtained experimentally. Note that this is not relevant for β and g$_2$, which have only one hydrogen. For the α carbon, for which a considerable forking of 0.105 is experimentally seen, the following 5-step scale was used:

>   **0 ( ):** The distance D between the dots (that mark the measurement-time-weighted averages in Fig. 5) was $0.08 < D < 0.13$ units for all the calculated OPs (that is, for all different lipids).
>
>   **1 (F):** $(0.06 < D < 0.08)$ OR $(0.13 < D < 0.15)$.
>
>   **2 (F):** $(0.04 < D < 0.06)$ OR $(0.15 < D < 0.17)$.
>
>   **3 (F):** $(0.02 < D < 0.04)$ OR $(0.17 < D < 0.19)$.
>
>   **4 (F):** $(D < 0.02)$ OR $(0.19 < D)$.
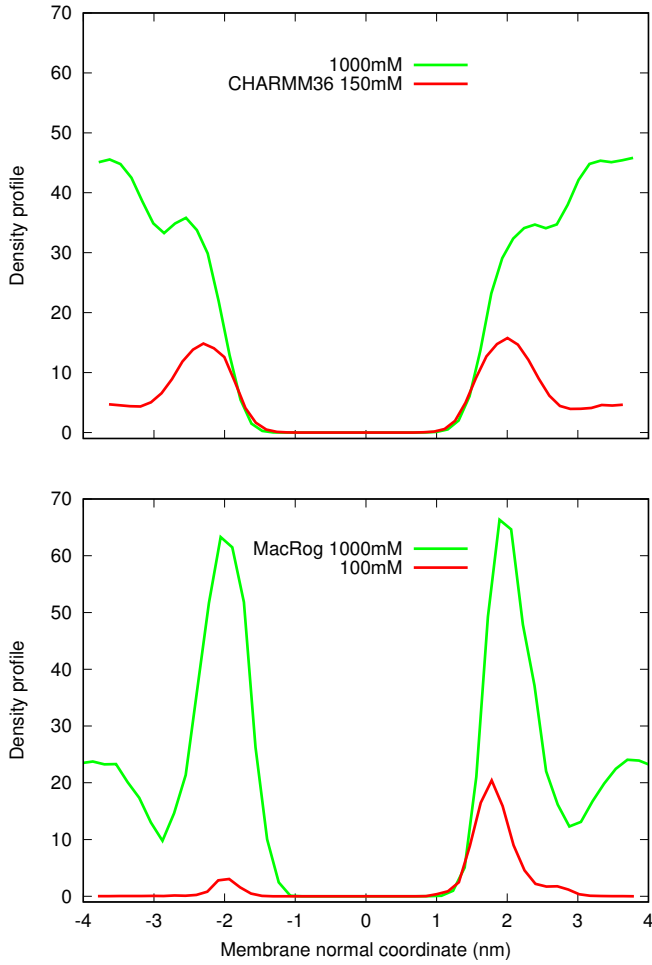
FIG. 12: Ca2+ density profiles from simulations.

29.Ca2+ binding in CHARMM is lower than to neutral membrane. The reason should be found out (probably equilibration). 30.These are now mass densities, numbers would be probably better. 31.Counterions should be also included. 32.Not all the data from MacRog is included.

For the g_3 carbon, for which no forking is indicated by experiments, the following 5-step scale was used:

0 ( ): $D < 0.02$.

1 (F): $0.02 < D < 0.04$.

2 (F): $0.04 < D < 0.06$.

3 (F): $0.06 < D < 0.08$.

4 (F): $0.08 < D$.

For the g_1 carbon, for which a considerable forking of 0.13 is experimentally seen, the following 5-step scale was used:

0 ( ): $0.11 < D < 0.15$.
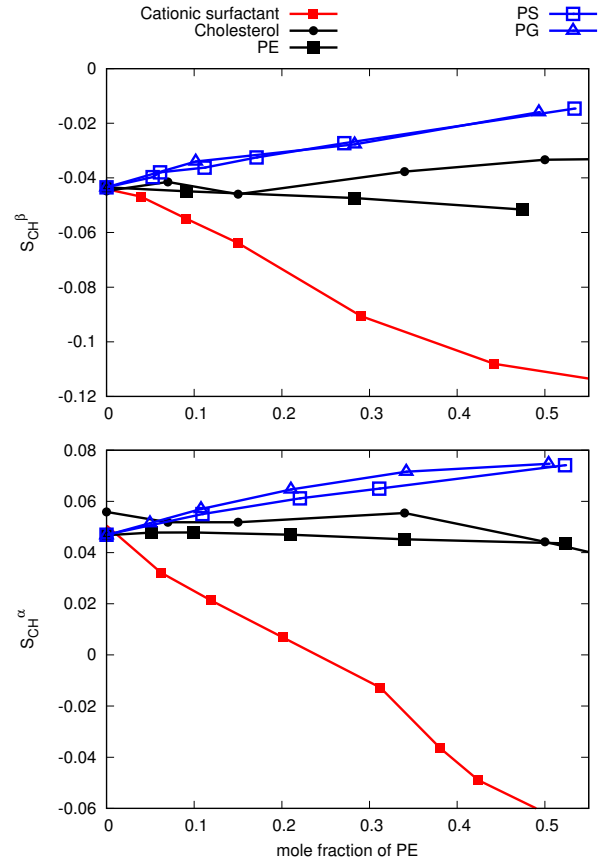
FIG. 13: PC headgroup order parameters from experiments of mixtures with PE, PS, PG and cholesterol [18, 41, 51]. Signs are determined as discussed in [9, 11].

1 (F): $(0.09 < D < 0.11)$ OR $(0.15 < D < 0.17)$.

2 (F): $(0.07 < D < 0.09)$ OR $(0.17 < D < 0.19)$.

3 (F): $(0.05 < D < 0.07)$ OR $(0.19 < D < 0.21)$.

4 (F): $(D < 0.05)$ OR $(0.21 < D)$.

Based on these assessments of magnitude and forking deviations, each carbon was then assigned to one of the following groups: "within experimental error" (magnitude and forking deviations both on step 0 of the scales described above), "almost within experimental error" (sum of the magnitude and forking deviation steps 1 or 2), "clear deviation from experiments" (sum of magnitude and forking deviation steps from 3 to 5), and "major deviation from experiments" (sum of magnitude and forking deviation steps from 6 to 8). These groups are indicated by colors in Fig. 4. (Note that for β and g_2, for which there can be no forking, the corresponding group assignment limits were: 0, 1, 2, and 3.)

Finally, the total ability of the force field to describe the headgroup and glycerol structure was estimated. To this end, the groups were given the following weights: 0 (within experimental error), 1 (almost within experimental error), 2 (clear
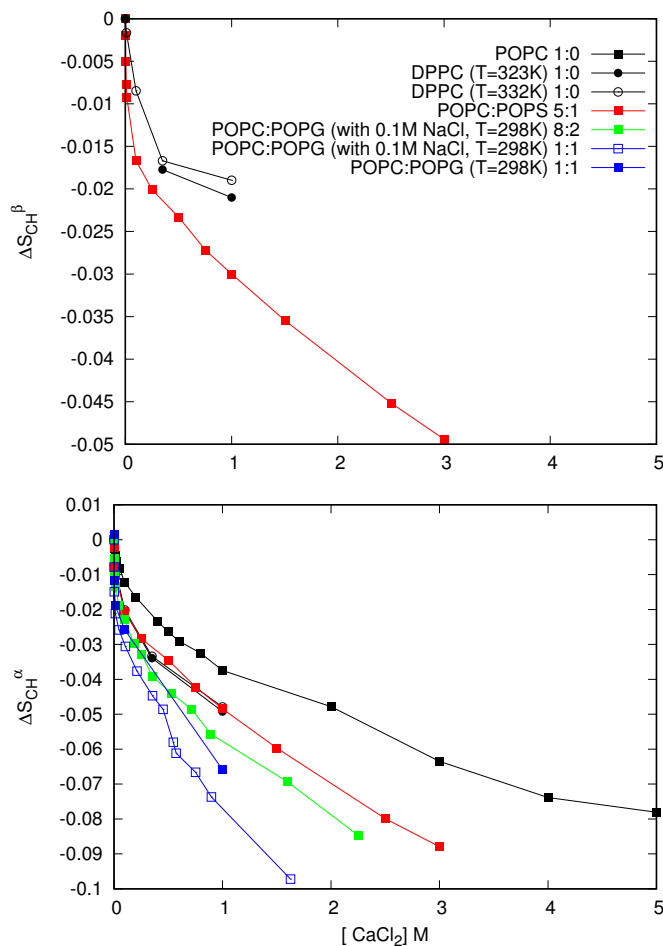
FIG. 14: The change of PC headgroup order parameters as a function of $CaCl_2$ measured from bilayers containing different amount of negatively charged lipids. The values are taken from 2H NMR experiments reported in the literature (DPPC [52], POPC [53], POPC:POPS (5:1) [7], POPC:POPG mixtures with 0.1M NaCl [50] and POPC:POPG (1:1) without NaCl [49]). As expected, the decrease of order parameters with the added $CaCl_2$ is more pronounced for systems with larger fraction of negatively charged lipids, indicating larger amount amount of bound cations.

FIG. 15: The response of headgroup order parameters to the fixed amount of cationic surfactants in POPC bilayer is compared between simulations and experiments [51].

deviation from experiments), 4 (major deviation from experiments), and the weights of the five carbons were summed up. The sum, given in the Σ-column of Fig. 5, was then used to (roughly and subjectively, as should be clear from the above description) rank the force fields.
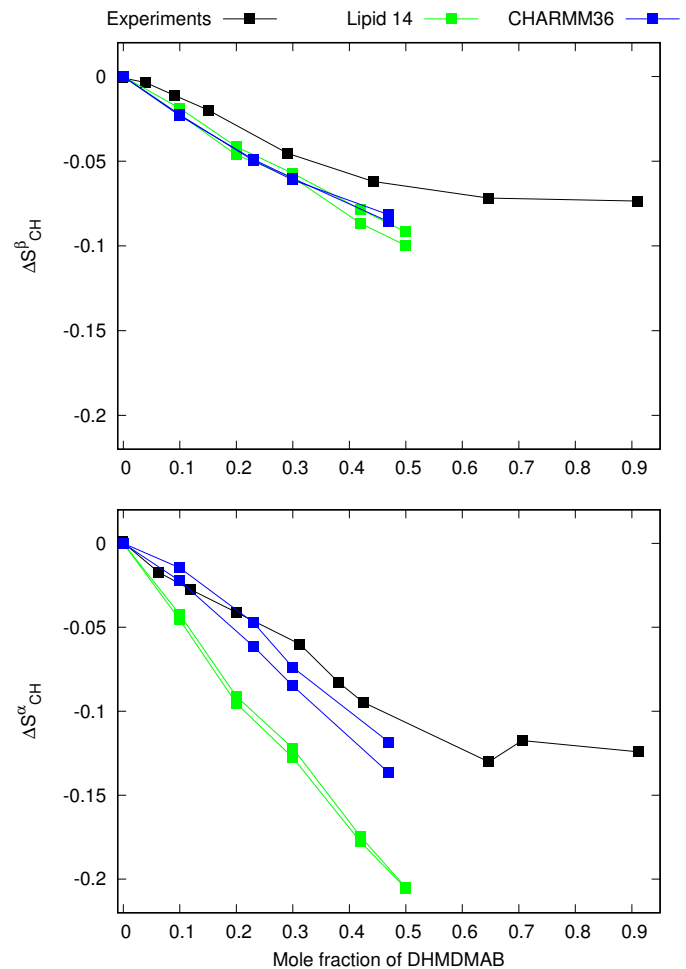
* samuli.ollila@helsinki.fi

[1] M. A. Lemmon, Nat. Rev. Mol. Cell Biol. **9**, 99 (2008).
[2] P. A. Leventis and S. Grinstein, Annual Review of Biophysics **39**, 407 (2010).
[3] L. Li, X. Shi, X. Guo, H. Li, and C. Xu, Trends in Biochemical Sciences **39**, 130 (2014), ISSN 0968-0004.
[4] T. Yeung, G. E. Gilbert, J. Shi, J. Silvius, A. Kapus, and S. Grinstein, Science **319**, 210 (2008).
[5] H. Zhao, E. K. J. Tuominen, and P. K. J. Kinnunen, Biochemistry **43**, 10302 (2004).
[6] G. P. Gorbenko and P. K. Kinnunen, Chemistry and Physics of Lipids **141**, 72 (2006).
[7] M. Roux and M. Bloom, Biochemistry **29**, 7077 (1990).
[8] A. Melcrová, S. Pokorna, S. Pullanchery, M. Kohagen, P. Jurkiewicz, M. Hof, P. Jungwirth, P. S. Cremer, and L. Cwiklik, Sci. Reports **6**, 38035 (2016).
[9] A. Botan, F. Favela-Rosales, P. F. J. Fuchs, M. Javanainen, M. Kanduč, W. Kulig, A. Lamberg, C. Loison, A. Lyubartsev, M. S. Miettinen, et al., J. Phys. Chem. B **119**, 15075 (2015).
[10] A. Catte, M. Girych, M. Javanainen, C. Loison, J. Melcr, M. S.
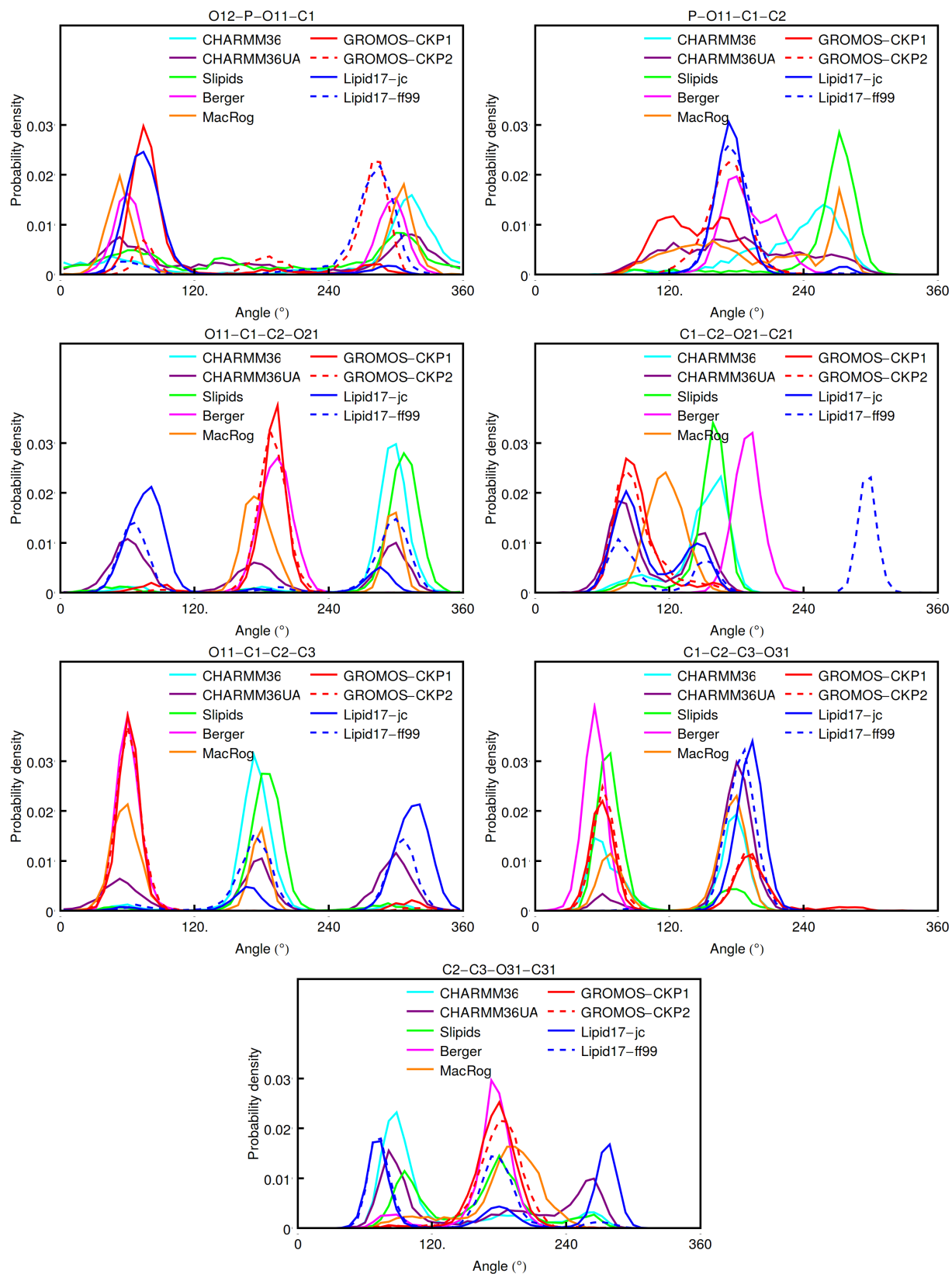
FIG. 16: Dihedral angle distributions of bonds from phosphate to acyl chain carbonyls from different simulation models.
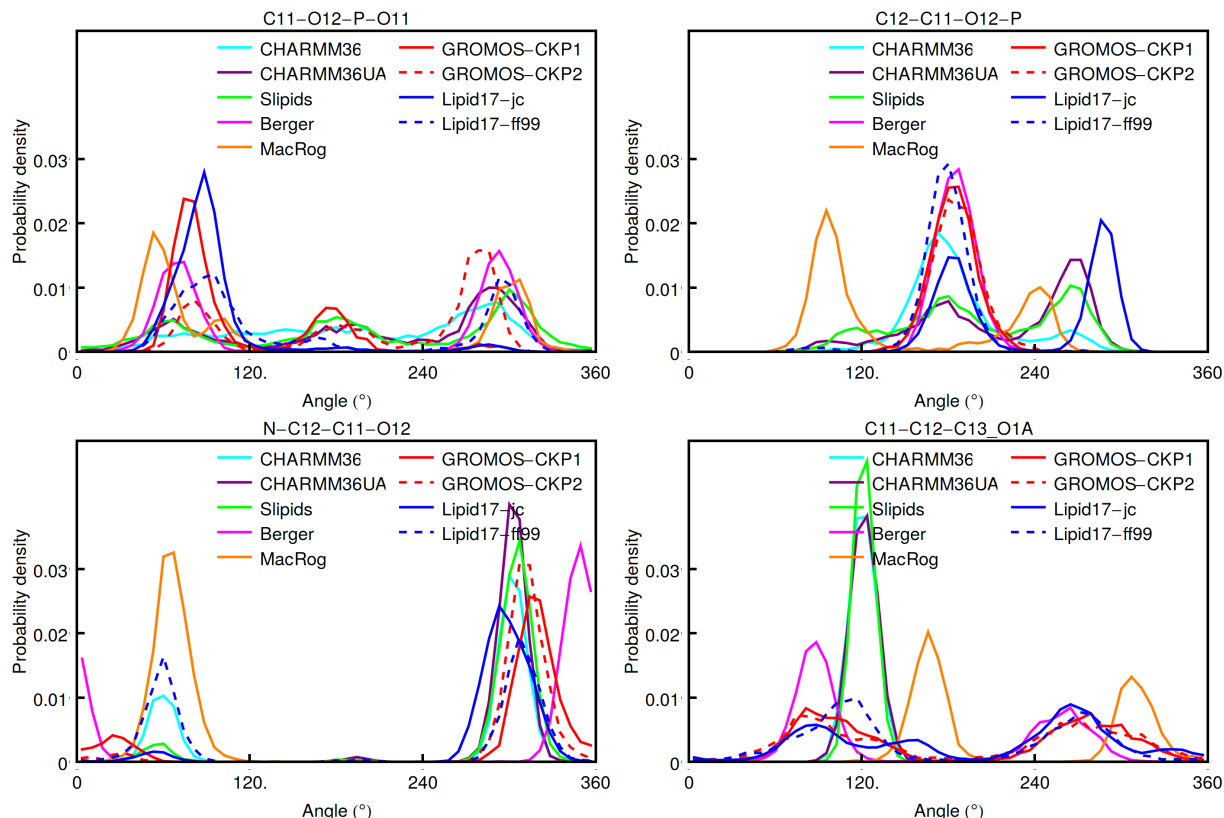
FIG. 17: Dihedral angle distributions of bonds from phosphate to headgroup from different simulation models.

Miettinen, L. Monticelli, J. Maatta, V. S. Oganesyan, O. H. S. Ollila, et al., Phys. Chem. Chem. Phys. **18**, 32560 (2016).

[11] O. S. Ollila and G. Pabst, Biochimica et Biophysica Acta (BBA) - Biomembranes **1858**, 2512 (2016).

[12] J. Seelig, Cell Biology International Reports **14**, 353 (1990), ISSN 0309-1651, URL http://www.sciencedirect.com/science/article/pii/030916519091204H.

[13] C. G. Sinn, M. Antonietti, and R. Dimova, Colloids and Surfaces A: Physicochemical and Engineering Aspects **282-283**, 410 (2006), a Collection of Papers in Honor of Professor Ivan B. Ivanov (Laboratory of Chemical Physics and Engineering, University of Sofia) Celebrating his Contributions to Colloid and Surface Science on the Occasion of his 70th Birthday.

[14] P. T. Vernier, M. J. Ziegler, and R. Dimova, Langmuir **25**, 1020 (2009).

[15] J. M. Boettcher, R. L. Davis-Harrison, M. C. Clay, A. J. Nieuwkoop, Y. Z. Ohkubo, E. Tajkhorshid, J. H. Morrissey, and C. M. Rienstra, Biochemistry **50**, 2264 (2011).

[16] T. M. Ferreira, R. Sood, R. Bärenwald, G. Carlström, D. Topgaard, K. Saalwächter, P. K. J. Kinnunen, and O. H. S. Ollila, Langmuir **32**, 6524 (2016).

[17] H. U. Gally, G. Pluschke, P. Overath, and J. Seelig, Biochemistry **20**, 1826 (1981).

[18] P. Scherer and J. Seelig, EMBO J. **6** (1987).

[19] T. Piggot, *CHARMM36 DOPS simulations (versions 1 and 2) 303 K 1.0 nm LJ switching* (2017), URL https://doi.org/10.5281/zenodo.1129411.

[20] T. Piggot, *CHARMM36-UA DOPS simulations (versions 1 and 2) 303 K 1.0 nm LJ switching* (2017), URL https://doi.org/10.5281/zenodo.1129456.

[21] J. P. M. Jämbeck and A. P. Lyubartsev, Phys. Chem. Chem. Phys. **15**, 4677 (2013).

[22] T. Piggot, *Slipids DOPS simulations (versions 1 and 2) 303 K 1.0 nm cut-off with LJ-PME* (2017), URL https://doi.org/10.5281/zenodo.1129439.

[23] F. Favela-Rosales, *MD simulation trajectory of a fully hydrated DOPS bilayer: SLIPIDS, Gromacs 5.0.4. 2017.* (2017), URL https://doi.org/10.5281/zenodo.495510.

[24] P. Mukhopadhyay, L. Monticelli, and D. P. Tieleman, Biophysical Journal **86**, 1601 (2004).

[25] T. Piggot, *Berger DOPS simulations (versions 1 and 2) 303 K 1.0 nm cut-off* (2017), URL https://doi.org/10.5281/zenodo.1129419.

[26] T. Piggot, *GROMOS-CKP DOPS simulations (versions 1 and 2) 303 K with Berger/Chiu NH3 charges and PME* (2017), URL https://doi.org/10.5281/zenodo.1129429.

[27] T. Piggot, *GROMOS-CKP DOPS simulations (versions 1 and 2) 303 K with GROMOS NH3 charges and PME* (2017), URL https://doi.org/10.5281/zenodo.1129447.

[28] T. Piggot, *CHARMM36 POPS simulations (versions 1 and 2) 298 K 1.0 nm LJ switching* (2017), URL https://doi.org/10.5281/zenodo.1129415.

[29] T. Piggot, *CHARMM36 POPS simulations (versions 1 and 2) 298 K 1.0 nm LJ switching with K ions* (2018), URL https://doi.org/10.5281/zenodo.1182654.

[30] T. Piggot, *CHARMM36-UA POPS simulations (versions 1 and 2) 298 K 1.0 nm LJ switching* (2017), URL https://doi.org/10.5281/zenodo.1129458.

[31] T. Piggot, *Slipids POPS simulations (versions 1 and 2) 298 K 1.0 nm cut-off with LJ-PME* (2017), URL https://doi.

org/10.5281/zenodo.1129441.

[32] T. Piggot, *Berger POPS simulations (versions 1 and 2) 298 K 1.0 nm cut-off* (2017), URL https://doi.org/10.5281/zenodo.1129425.

[33] A. Maciejewski, M. Pasenkiewicz-Gierula, O. Cramariuc, I. Vattulainen, and T. Róg, J. Phys. Chem. B **118**, 4571 (2014).

[34] M. Javanainen, *Simulation of a pops bilayer* (2017), URL https://doi.org/10.5281/zenodo.1120287.

[35] T. Piggot, *GROMOS-CKP POPS simulations (versions 1 and 2) 298 K with Berger/Chiu NH3 charges and PME* (2017), URL https://doi.org/10.5281/zenodo.1129431.

[36] T. Piggot, *GROMOS-CKP POPS simulations (versions 1 and 2) 298 K with GROMOS NH3 charges and PME* (2017), URL https://doi.org/10.5281/zenodo.1129435.

[37] J. B. Klauda, R. M. Venable, J. A. Freites, J. W. O'Connor, D. J. Tobias, C. Mondragon-Ramirez, I. Vorobyov, A. D. MacKerell Jr, and R. W. Pastor, J. Phys. Chem. B **114**, 7830 (2010).

[38] O. H. S. Ollila, *POPS+83%popc lipid bilayer simulation at T298K ran CHARMM_GUI force field and Gromacs* (2017), URL https://doi.org/10.5281/zenodo.1011104.

[39] M. Roux and M. Bloom, Biophys. J. **60**, 38 (1991).

[40] J. L. Browning and J. Seelig, Biochemistry **19**, 1262 (1980).

[41] T. M. Ferreira, F. Coreta-Gomes, O. H. S. Ollila, M. J. Moreno, W. L. C. Vaz, and D. Topgaard, Phys. Chem. Chem. Phys. **15**, 1976 (2013).

[42] R. Wohlgemuth, N. Waespe-Sarcevic, and J. Seelig, Biochemistry **19**, 3315 (1980).

[43] G. Büldt and R. Wohlgemuth, The Journal of Membrane Biology **58**, 81 (1981), ISSN 1432-1424, URL http://dx.doi.org/10.1007/BF01870972.

[44] M. Roux and J.-M. Neumann, FEBS Letters **199**, 33 (1986).

[45] S. A. Pandit and M. L. Berkowitz, Biophysical Journal **82**, 1818 (2002).

[46] U. R. Pedersen, C. Leidy, P. Westh, and G. H. Peters, Biochimica et Biophysica Acta (BBA) - Biomembranes **1758**, 573 (2006).

[47] J. Pan, X. Cheng, L. Monticelli, F. A. Heberle, N. Kucerka, D. P. Tieleman, and J. Katsaras, Soft Matter **10**, 3716 (2014).

[48] J. Seelig, P. M. MacDonald, and P. G. Scherer, Biochemistry **26**, 7535 (1987).

[49] F. Borle and J. Seelig, Chemistry and Physics of Lipids **36**, 263 (1985).

[50] P. M. Macdonald and J. Seelig, Biochemistry **26**, 1231 (1987).

[51] P. G. Scherer and J. Seelig, Biochemistry **28**, 7720 (1989).

[52] H. Akutsu and J. Seelig, Biochemistry **20**, 7366 (1981).

[53] C. Altenbach and J. Seelig, Biochemistry **23**, 3913 (1984).

ToDo